# Characterization of Corrosion Product of Warm Deformed 316LN Steel

Viranshu kumar[1*], Manohar Kumar Singh[1]

[1] ICFAI University, Ranchi-835222

**Abstract** The materials used for this investigation was austenitic stainless steel of grade 316LN. Specimens were placed in simulated primary water environment after deformation. The corrosion behaviour was investigated using OCP and EIS tests. After corrosion tests metallographic examinations were performed using scanning electron microscope also characterization of corrosion product was done by XRD and Raman spectroscopy. The EIS curve shows that the rate of corrosion increasers after 50% deformation due to the destruction of protective oxide film of chromium. XRD results showed the presence of ϒ-$Fe_2O_3$, α-FeOOH and ϒ- FeOOH which is responsible for the formation of passive layer on the surface of specimen. It is evident from the diffractograms that the rust of steel 316LN invariably exhibit very strong peaks of α-FeOOH (goethite) and γ -$Fe_2O_3$ (maghemite) in test solutions. It is seen from the Raman shifts recorded, the majority of peaks are attributed to α-FeOOH (goethite) and γ -$Fe_2O_3$ (maghemite). In contrast to this, the rusts formed on 50% deformed samples are mostly γ -FeOOH (lepidocrocite).

**Keywords: -** Austenitic stainless steel, corrosion, scanning electron microscope, deformation.

## Introduction

One of the most frequently used steels is austenitic stainless steel (ASS) due to its strong corrosion resistance, high thermal stability, excellent weldability, and superior impact toughness. One of the important drawback of these steels are relatively low yield strength (~250–350 MPa) in annealing condition which restricting the usage of these materials in structural applications [1-4]. There are various strengthening mechanisms for Austenic stainless steel, such as grain refining, and work hardening. Among different strengthening mechanisms, grain refinement is considered as the appropriate and convenient method which increases strength with less compensation of ductility. Hence, there is great interest on developing nano/ultrafine grained austenitic stainless steels [5]. Stainless steel is a corrosion resistant material due to formation of protective oxide film of chromium on the surface. It is used in primary and pressurized water reactor in nuclear plants due to superior corrosion, metallurgical properties and mechanical strength [6-11]. Stainless steel exhibit excellent mechanical properties and reasonable corrosion resistance in different environment but it lost their properties for long service period at high temperature and highly corrosive environment [11-20]. For improving the high temperature mechanical strength and corrosion resistance stainless steels are subjected to deformation process like Sever Plastic Deformation,

forging and rolling. Mechanical and metallurgical properties of steel can be improved by producing ultra-fine, nano size grain with the help of deformation [20].

**Experimental Procedure**

**Material and Methods**

The 316LN austenitic stainless steel has been used for this investigation. The 316LN steel billets with a dimension of 50 by 30 by 8 $mm^3$ were subjected to 20 to 50 % deformation by a warm deformation process using a 150-ton hydraulic press at 700°C and cooled in air after deformation. After the warm forging, some forged samples were annealed at 1,070°C and 950°C for 2 h and cooled in water and a furnace, respectively. The corrosion resistance of sample was performed in simulated primary water environment (PWRE). Current response as a function of frequency was measured by the help of electrochemical impedance spectroscopy (EIS) Test. Characterization of corrosion product were performed using XRD and Raman Spectroscopy.

**Result and Discussion**

**Corrosion study of Deformed Austenitic Steel**

All the electrochemical tests were repeated at least three times to confirm the reproducibility. OCP measures the free corrosion potential or equilibrium potential of the working electrode with respect to a reference electrode in an open circuit. The corrosion potential is moderated by the rate of oxidation and reduction due to the chemical reaction at the interface of the working electrode and electrolyte. We have, therefore, measured the OCP of the 316LN stainless steel. During the measurements, it was allowed one hour to attain the equilibrium potential and the fluctuation limit in the data within ± 10 mV is considered as a stable potential. The OCP measurements in PWRE solution indicated that the stabilized potential of 316LN sample is -410 $mV_{SCE}$.

**Electrochemical Impedance Spectroscopy (EIS) Study**

In order to understand the corrosion behavior and the prevailing mechanism for the electrochemical reaction at the steels and electrolyte interface, the impedance test was carried out. The impedance analysis is governed by Bode and Nyquist impedance curves. Therefore in simple way, from the Bode impedance plot we can calculate the polarization resistance of the 316LN. The average polarization resistance for the 316LN is 19788 $ohm.cm^2$. Nyquist impedance is a plot between real parts of impedance versus the imaginary part, characterized by semicircle shape. The total diameter of the Nyquist plot represents the resistance offered by the metal surface towards electrochemical degradation and also the nature of curve is very important to understand the mechanism of corrosion. Nyquist impedance is a plot between real parts of impedance versus the imaginary part, characterized by semicircle shape.

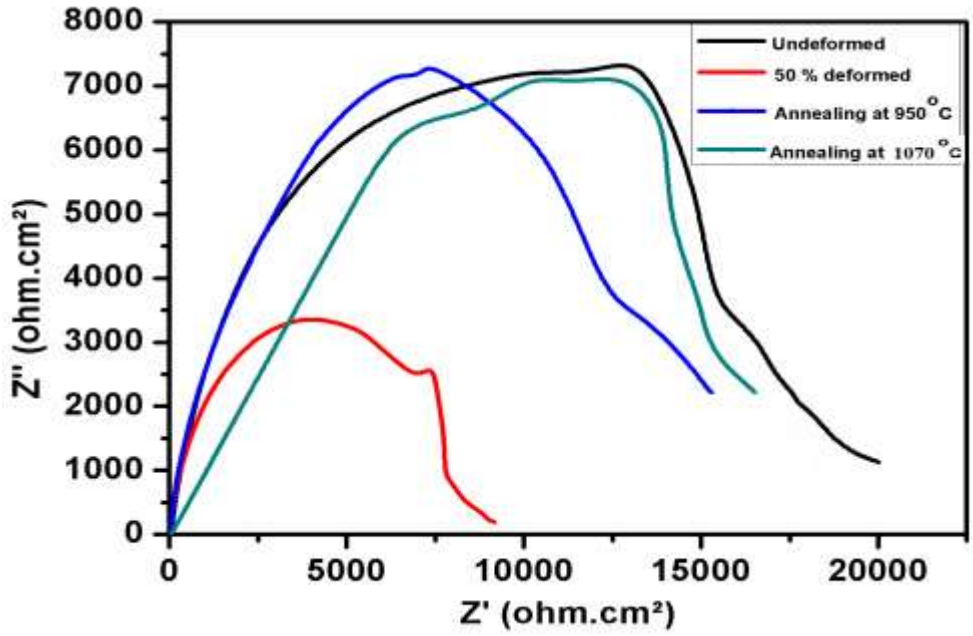


**Figure 1:** Nyquist plot of 316LN, 50% deformed, annealing at 950ºC and annealing at 1070ºC steel

For example, the semicircle type of curve indicates pure resistance (R) and capacitance (C) behavior whereas the semicircle associated with linear line at 45º phase angle indicates the Warburg (W) contribution. It is clear from the diagram that the diameter of the substrates follows the order; undeformed > annealing at 1070ºC > annealing at 950ºC > 50 % deformed. So the resistance offered by the Steel 316LN is more than the 50 % deformed steel.

**Raman Spectroscopy Studies**

A vast difference in corrosion rate of steels and adherence of rusts to their surfaces in different types of test electrolytes was quite an interesting observation and led us to investigate this further by determining the nature of rusts and their morphology. Rusts collected from different samples after completions of the experiments were subjected to Raman spectroscopy and spectra are shown in Figure 2. It is important to mention here that certain structures of iron oxides are recognized more protective than the others. Thus, lepidocrocite (γ-FeOOH), akaganeite (β-FeOOH), iron hydroxide (FeOOH), etc. are reported unstable and non-protective oxides. Due to their instability (tendency to transform to other stable forms of oxide) and pores morphology, they act as cathodic depolarizers and reservoir for moisture, oxygen and polluting gases. On the other hand some other phases of oxides such as maghemite (γ- $Fe_2O_3$), goethite (α-FeOOH), etc. are quite stable and bear a compact morphology. It is seen from the Raman shifts recorded in Figure 2, the majority of peaks at are attributed to α-FeOOH (goethite) and γ -$Fe_2O_3$ (maghemite). In contrast to this, the rusts formed on 50% deformed samples are mostly γ -FeOOH (lepidocrocite).These phases of rusts are unstable and porous in nature and transform to other form of oxides with passage of time and depolarize the cathodic reactions.

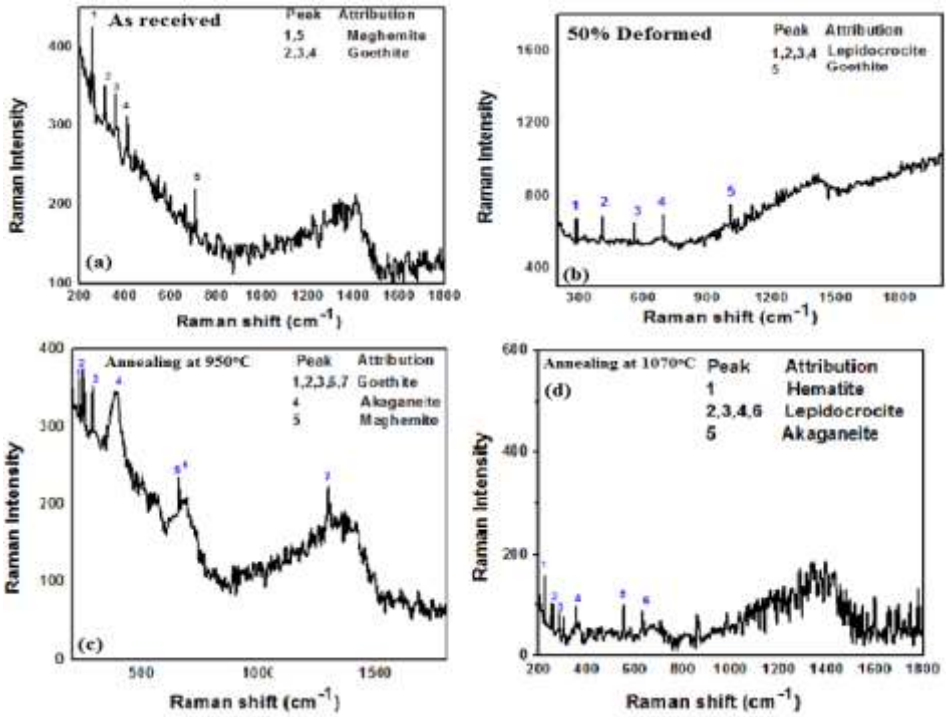


**Figure 2** Raman spectra of 316LN Steel surface immersed PWR Environment

**X-ray diffraction studies**

The study of rusts by Raman spectroscopy as described above has provided important clue about the nature of rusts formed on steels surfaces exposed under different conditions. Unfortunately, the Raman shifts of many compounds are either very closer or tally with each other. For example, some of the researcher reported that strongest peak of maghemite at 670 and 486 $cm^{-1}$. On the other hand some of the author reported the Raman peak at 670 $cm^{-1}$ corresponding to ferroxyhite. This occurs as many compounds bear identical bond polarizability, crystal symmetry and the exciting wave length resulting in the same Raman shift. Further, the Raman peaks in the range of 1300–1314 $cm^{-1}$ exhibit different iron oxides phases. Thus depending only on one characterization technique may lead to an erroneous conclusion. It was therefore necessary to use technique other than Raman spectroscopy to arrive at a definite conclusion about the phases present in the corrosion products. In view of this X-ray diffraction studies of the generated corrosion products were performed and diffraction patterns are shown in Figure 3. It is evident from the diffractograms that the rust of as received invariably exhibit very strong peaks of α -FeOOH (goethite) and γ -$Fe_2O_3$ (maghemite) in test solutions, however, stronger peaks of γ -FeOOH (lepidocrocite) are noted for the 50% deformed sample. This is in conformity with the results recorded by Raman spectroscopy.

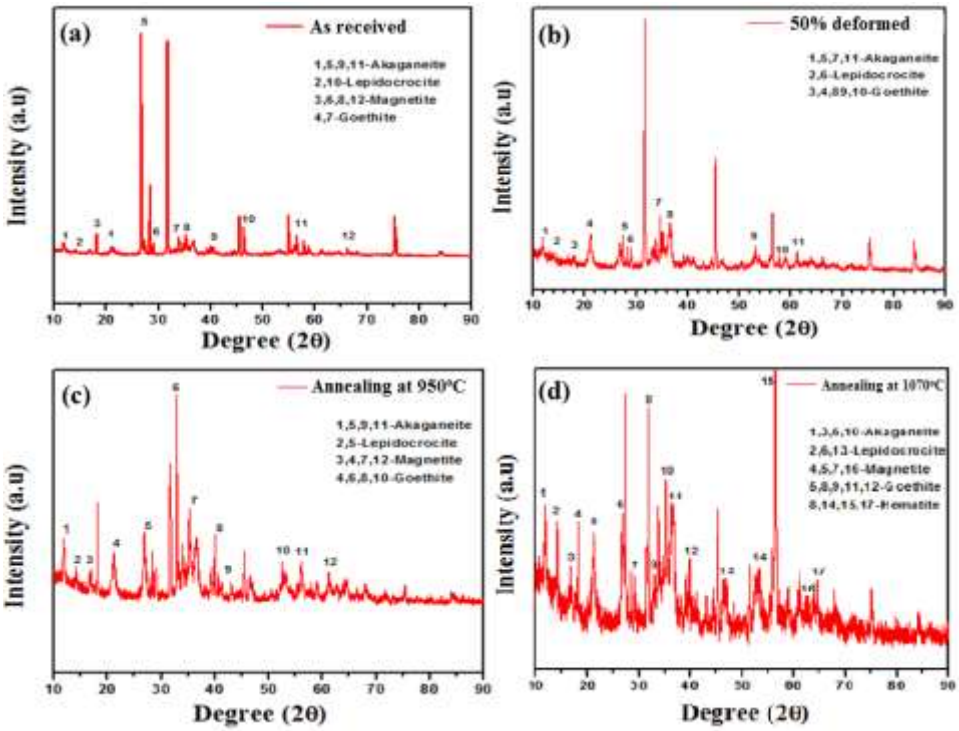


**Figure 3** XRD spectra of 316LN steel surface immersed in the PWR solution

**Characterization of Passive Layer Developed on Steel Rebars in PWRE solution**

The image shows the presence of a great amount of corrosion products dispersed over the entire surface of the steel. The analysis of the cross section of the same film shows the presence of an oxide film with heterogeneous thickness ranging between 0.5 and 1 µm.

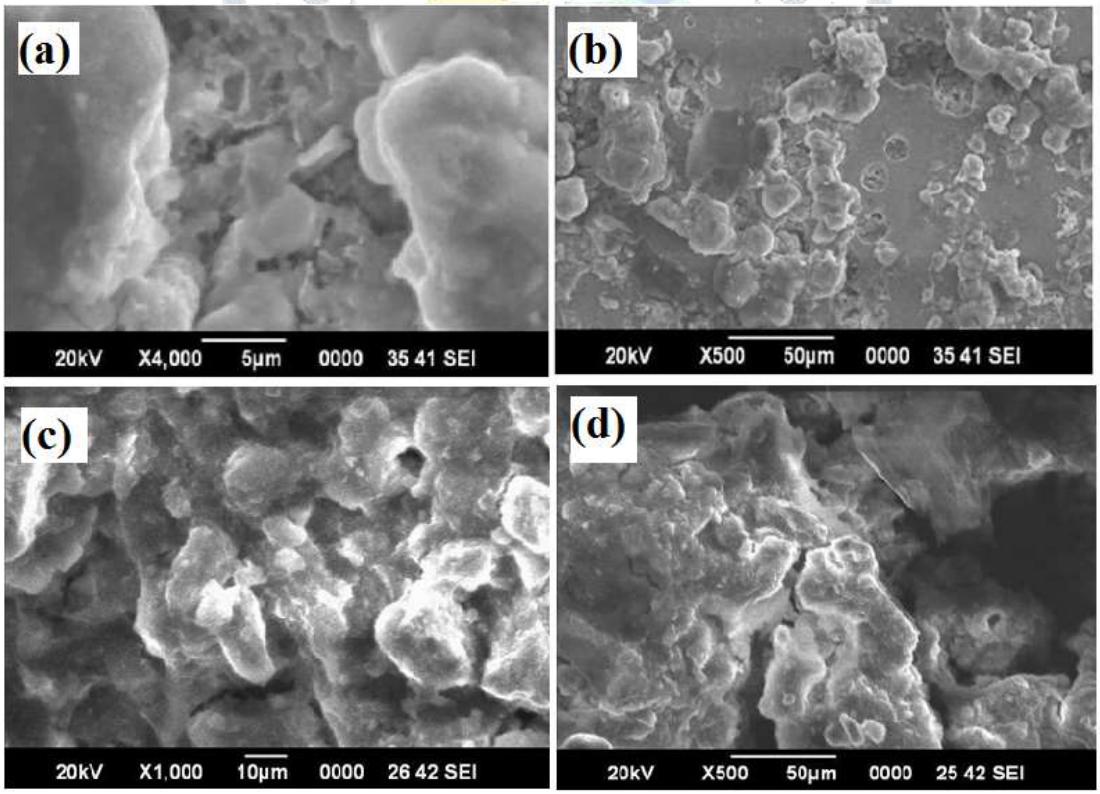


**Figure 4** SEM image of 316LN Steel surface immersed in the PWR solution

The characterization of passive layer developed on steel under PWR solution environment was carried out. The constituent compound analysis as well as growth of passive layer was investigated under both conditions. SEM was employed to observe the passive layer around the surface of the steel and images were taken at different resolutions as shown in Figures 4. These images proved to be very helpful to reveal the interface of the steel where passive layer is developed. It was observed that the surface of steel bar which seemed very smooth at macro level was still very non-uniform at micro and nano level which definitely affects the quality of passive layer.

**Conclusions**

In this investigation, an attempt has been made to develop the optimum corrosion resistance without sacrificing the strength of austenitic stainless steel by modifying the microstructure with the help of warm forging followed by annealing. The results obtained are as follows:

1. Warm forging followed by annealing treatment gives optimum corrosion resistance in a corrosive environment because of the formation of homogeneous microstructure.
2. Grain refinement occurs after increasing the percentage of deformation, but after annealing of warm forged sample, microstructural refinement occurs due to the formation of homogeneous and equiaxed strain-free austenite grains. From the obtained result, we also concluded that annealing at $1070^{O}C$ after 50% deformation gives the higher strength without sacrificing the corrosion resistance.
3. XRD results showed the presence of $\Upsilon$-$Fe_2O_3$, α-FeOOH and $\Upsilon$- FeOOH which is responsible for the formation of passive layer on the surface of specimen. It is evident from the diffractograms that the rust of steel 316LN invariably exhibit very strong peaks of α-FeOOH (goethite) and γ -$Fe_2O_3$ (maghemite) in test solutions. For Steel 316LN, however, stronger peaks of γ -FeOOH (lepidocrocite) are noted. This is in conformity with the results recorded by Raman spectroscopy.

**References**


1. Michael F. McGuire, “Stainless Steels for Design Engineers,” ASM International (2008): 296, ISBN: 978-0-87170-717-8.
2. K.H. Lo, C.H. Shek, J.K.L. Lai, “Recent developments in stainless steels”, Mater. Sci. Eng. R. 65 (2009) 39–104.
3. S. J. Zinkle, G. S. Was, “Materials challenges in nuclear energy,” Acta Materials 6 (2013): 735-758. https://doi.org/10.1016/j.actamat.2012.11.004
4. T. Allen, J. Busby, M. Meyer, D. Petti, “Materials challenges for nuclear systems,” Materials Today 13 (2010): 14–23. https://doi.org/10.1016/S1369-7021(10)70220-0
5. Viranshu kumara , Ratnesh Kumar Gupta, Ghanshyam Das, Influence of Deformation and Annealing on Microstructure and Corrosion Behavior of Austenitic Stainless Steel, Materials Today: Proceedings 22 (2020) 3347–3352, https://doi.org/10.1016/j.matpr.2020.03.361
6. V. Kumar, R. Gupta, and G. Das, "Effect of Warm Forging on the Microstructure and Corrosion Behavior of Austenitic Stainless Steel 316LN," *Materials Performance and Characterization* 9, no. 1 (2020): 94-106. https://doi.org/10.1520/MPC20190228
7. Kumar, V., Gupta, R.K. & Das, G. Influence of Forging and Annealing on the Microstructure and Corrosion Behavior of Austenitic Stainless Steel. J. Inst. Eng. India Ser. D 101, 105–109 (2020). https://doi.org/10.1007/s40033-020-00209-2

8. Viranshu Kumar, Ratnesh Kumar Gupta and Ghanshyam Das, Pitting and Electrochemical corrosion behaviour of 316L austenitic stainless steel subjected to warm deformation, IOP Conference Series: Materials Science and Engineering, Volume 653, International Conference on Advances in Materials and Manufacturing Engineering 15–19 March 2019, Kalinga Institute of Industrial Technology (Deemed to be University), Bhubaneswar, India.
9. S. K. Ghosh, Shikhar Jha, P. Mallick, P. P. Chattopadhyay, "Influence of Mechanical Deformation and Annealing on Kinetics of Martensite in a Stainless Steel," Materials and Manufacturing Processes, 28 (Augest 2013): 249–255. https://doi.org/10.1080/ 10426914.2012.667893
10. Yinghui Zhoua, Yongchang Liua, Xiaosheng Zhoua, "Precipitation and hot deformation behavior of austenitic heat-resistant steels: A review," Journal of Materials Science & Technology 33, 12 (December 2017): 1448-1456. https://doi.org/10.1016/j.jmst. 2017.01.025
11. Olson, G. B. Cohen M, "A mechanism for the strain-induced nucleation of martensitic transformations", Journal of Less Common Metals 28, 1 (July 1972): 107–118. https://doi.org/10.1016/0022-5088(72)90173-7
12. M Odnobokova, A Kipelova, A Belyakov and R Kaibyshev, "Microstructure evolution in a 316L stainless steel subjected to multidirectional forging and unidirectional bar rolling," IOP Conf. Series: Materials Science and Engineering 63 (2014) 012060. https://doi:10.1088/1757-899X/63/1/012060
13. Xinyun Wang, Daokuan Wang, Junsong Jin, Jianjun Li, "Effects of strain rates and twins evolution on dynamic recrystallization mechanisms of austenite stainless steel," Materials Science & Engineering A 761 (July 2019): 138044. https://doi.org/10.1016/j. msea.2019.138044
14. Tian-Sheng Hung, Wen-Ta Tsai, Szu-Jung Pan, Keh-Chin Chang, "Pitting corrosion Behavior of 2101 duplex stainless steel in chloride solution," Corrosion engineering science and technology 53 (July 2018): 9-15. https://doi.org/10.1080/1478422X.2017
15. Yueling Guo, En-Hou Han, Jianqiu Wang, "Effects of Forging and Heat Treatments on the micro structure and oxidation behavior of 316LN Stainless Steel in High Temperature Water," Journal of Materials Science & Technology, 31 (2015): 403-412. https://doi.org/ 10.1016/j.jmst.2014.08.014
16. S. K. Ghosh, Shikhar Jha, P. Mallick, P. P. Chattopadhyay, "Influence of Mechanical Deformation and Annealing on Kinetics of Martensite in a Stainless Steel," Materials and Manufacturing Processes, 28 (Augest 2013): 249–255. https://doi.org/10.1080/ 10426914.2012.667893
17. Xingfei Xiea, Dong Ninga, "Stress corrosion cracking behavior of cold drawn 316 austenitic stainless steels in simulated PWR environment", Corrosion Science 112 (November 2016): 576–584. https://doi.org/10.1016/j. corsci.2016.08.014
18. Junjie Chen , Zhanpeng Lu, Qian Xiao, Xiangkun Ru, Guangdong Han , Zhen Chen , Bangxin Zhou, Tetsuo Shoji, "The effects of cold rolling orientation and water chemistry on stress corrosion cracking behavior of 316L stainless steel in simulated PWR water environments," Journal of Nuclear Materials, 472 (January 2016): 1-12. https://doi.org/ 10.1016/j.jnucmat.2016.01.018
19. Chio, J. Y, Jin W, "Strain induced martensite formation and its effect on strain hardening behavior in the cold drawn 304 austenitic stainless steels," Scripta Material 36 (January 1997): 99–104. https://doi.org/10.1016/S1359-6462(96)00338-7
20. Yinghui Zhoua, Yongchang Liua, Xiaosheng Zhoua, "Precipitation and hot deformation behavior of austenitic heat-resistant steels: A review," Journal of Materials Science & Technology 33, 12 (December 2017): 1448-1456. https://doi.org/10.1016/j.jmst. 2017.01.025